Optimal Landing of a Helicopter in Autorotation

Allan Y. Lee,* Arthur E. Bryson Jr.,† and William S. Hindson‡
Stanford University, Stanford, California

The landing of a helicopter in autorotation is formulated as a nonlinear optimal control problem with inequality constraints. The performance index is a weighted sum of the squares of vertical and horizontal velocity at touchdown. The control inequality constraint is a limit on the rotor thrust coefficient. The state inequality constraint is a limit on vertical sink rate. Optimal trajectories are calculated for initial conditions well within the height-velocity (H-V) restriction curve, with the helicopter in hover or forward flight. The optimal control history is similar to those used by helicopter pilots in autorotational landings. The study indicates that, subject to pilot acceptability, a substantial reduction could be made in the H-V restriction zone using optimal control techniques.

Introduction

GLIDING descent in autorotation is used by helicopter pilots in case of engine failure. A successful landing following an autorotation descent requires considerable skill, and since it is seldom practiced, it is considered quite dangerous. In fact, during certification, a region of low altitude and low velocity (the H-V restriction zone) is established where it is considered very difficult or impossible to make a safe landing.

Various methods and devices have been proposed to improve helicopter autorotational landing characteristics. One passive concept is to store energy in the helicopter main rotor by using blades with high inertia.[1,2] Active concepts, such as tip jets, flywheels, and auxiliary turbines, have also been explored.[3,4] Compared with these concepts of active energy addition and passive energy storage, the idea of optimal energy management as a means of improving safety has received relatively little attention. Using this idea, improved autorotation performance is achieved only by the management of available energy.

Johnson[5] used nonlinear optimal control theory to study the autorotative descent and landing of a helicopter in hover. He found that the optimal descent from hover is purely vertical. A comparison of the optimal control procedure with flight tests showed sufficient correlation to verify the basic features of the mathematical model used. We have extended the work of Johnson by adding inequality constraints on the thrust and the vertical velocity. Optimal trajectories were calculated for initial conditions within the H-V restriction curve, with the helicopter in hover or forward flight.

Dynamic Performance Model of a Helicopter in Autorotation

We used a point-mass model of an OH-58A light single-rotor helicopter modified with a High Energy Rotor System (HERS) in our study. The Bell Helicopter Co. conducted an autorotation flight test program [1,2] using this helicopter and obtained data suitable for comparison with analytical results of this research. A detailed description of the helicopter is given in Ref. 1; Table 1 summarizes the values of the model parameters used.

The model states are helicopter vertical and longitudinal velocities, vertical and longitudinal displacements (from the point at which engine failure occurred), and the rotor angular speed. Control variables were the vertical and longitudinal components of C_T, the rotor thrust coefficient. These can be related, approximately, to the pilot's collective and longitudinal cyclic controls. For example, the collective pitch control required to obtain this thrust may be obtained from blade element theory[5]

$$\theta_{75} = \frac{(1+\frac{3}{2}\mu^2)(6C_T/a\sigma) + \frac{3}{2}\lambda(1-\frac{1}{2}\mu^2)}{(1-\mu^2+9/4\mu^4)} \tag{1}$$

where θ_{75} is the rotor collective pitch angle at 75% span, and σ and a are the rotor solidity ratio and rotor blade two dimensional lift curve slope, respectively. The quantities μ and λ are, respectively, the advance and inflow ratios defined in the tip path plane.

With reference to Fig. 1, vertical and longitudinal force balances give

$$m\dot{w} = mg - T\cos\alpha + D\sin\theta \tag{2}$$

$$m\dot{u} = T\sin\alpha - D\cos\theta \tag{3}$$

where u,w are the (horizontal, vertical) components of the helicopter's velocity. u is defined positive forward and w positive downward. T is the rotor thrust and D the helicopter parasite drag. The torque balance equation of the helicopter's main rotor is

$$I_R\dot{\Omega} = -[\rho(\pi R^2)(\Omega R)^2 R]C_Q \tag{4}$$

where I_R is the total rotational inertia of the rotor system and C_Q the torque coefficient. It can be shown that the torque coefficient C_Q is the same as the power coefficient C_P.[6] In autorotation, C_P reflects the total effect of the induced, profile, and parasite power losses. In our study, C_P is approximated by

$$C_P = \tfrac{1}{8}\sigma\bar{c}_d + C_T\lambda \tag{5}$$

where $\bar{c}_d$ is the mean two dimensional profile drag coefficient of the rotor blades. The inflow ratio λ is defined in terms of the induced velocity v, which is modeled by

$$v = K_{ind}v_h f_I f_G \tag{6}$$

Received Sept. 19, 1986; revision received April 2, 1987.

*Presently with General Motors Research Laboratories, Warren, Michigan. Member AIAA.

†Paul Pigott, Professor of Engineering, Department of Aeronautics and Astronautics and Mechanical Engineering. Fellow AIAA.

‡Senior Research Associate, Department of Aeronautics and Astronautics. Member AIAA.

Table 1 Values of the parameters used in the point-mass model

S/No.	System parameter	Value used
1	f_e, equivalent flat plate area, ft^2	24.0
2	ρ, density of air, slug/ft^3	0.002378
3	σ, rotor solidity	0.048
4	R, radius of the main rotor, ft	17.63
5	δ_e, profile drag coefficient	0.0087
6	γ, rotor system Lock Number	2.61[a]
7	a, slope of 2-D blade lift coefficient w.r.t. the angle of attack	5.73
8	mg, weight of helicopter, lb. wt.	3000

[a] $\gamma = 2.61$, 3.19, 4.38 or 5.43.

where K_{ind} is the ratio of nonuniform inflow to uniform inflow induced power requirements. For the triangular downwash distribution assumed here, K_{ind} is given by $\frac{2}{5}(\sqrt{2})^3$, or approximately 1.13. v_h is the induced velocity at hover, and the induced velocity parameter f_I is given by the following expression[5]

$$f_I = \begin{cases} 1.0/\sqrt{(\bar{x}_2 + (\bar{x}_1 + f_I)^2)}, & \text{if } (2\bar{x}_1 + 3)^2 + \bar{x}_2^2 \geq 1.0 \\ \bar{x}_1(0.373\bar{x}_1^2 + 0.598\bar{x}_2^2 - 1.991) & \end{cases} \quad (7)$$

Otherwise, the parameters $\bar{x}_1$ and $\bar{x}_2$ are defined as follows

$$\bar{x}_1 = (u \sin\alpha - w \cos\alpha)/v_h \quad (8)$$

$$\bar{x}_2 = (u \cos\alpha + w \sin\alpha)/v_h \quad (9)$$

The first expression for f_I is the familiar momentum theory result. The second expression is our empirical approximation for the vortex-ring state (where the momentum theory breaks down). Since the vortex-ring state is a condition with high induced power loss, it is avoided during autorotation. The error introduced by the approximation should be minimal.

The power required for a helicopter to hover is reduced in ground effect. Therefore, the ground-effect parameter f_G in Eq. (6) always assumes a value less than unity. However, ground-based simulator experiments on the control of a helicopter in autorotation have shown that ground effect plays only a minor role in the overall autorotational performance of a helicopter. Ground effect is therefore neglected in our study and $f_G = 1$.

To justify the validity of the point-mass model, flight-test measurements of steady-state sink-rates of an OH-58A helicopter (with the HERS) in autorotation[2] were compared with those computed using this model. Figure 2 shows that the computed sink-rates compare well with the experimental data.

The kinematical relations are given simply by

$$\dot{h} = w \quad (10)$$

$$\dot{x} = u \quad (11)$$

Note that these relations are coupled only one-way to the dynamical relations. Since $h = h_0$ (height above ground at which engine fails) defines the final (landing) time for the optimal control problem, Eq. (10) is needed in its formulation. However, Eq. (11) may be removed, unless there is also a hard constraint on the terminal horizontal distance (e.g., when the helicopter is forced to land at a particular spot due to terrain considerations). Information on x may be recovered through the forward integration of Eq. (11) after the optimal time history of u has been found. (The constraint of landing at a specified spot was investigated briefly during the course of this research. See Sec. (4.6.4) of Ref. 10.)

Nondimensionalization and Scaling of the Optimal Control Problem

The computational efficiency and rate of convergence of numerical optimization methods depends critically on the

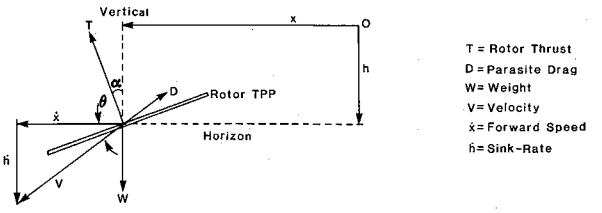

Fig. 1 Force balance diagram.

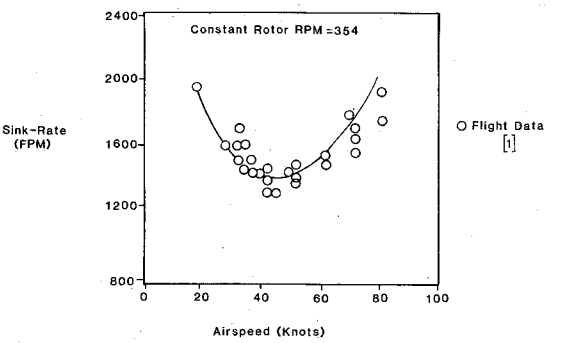

Fig. 2 Comparison of computed sink-rate with flight data.

scales used for the variables involved. This is especially true in nonlinear problems.[8] A "well scaled" problem is one in which a given order of magnitude change in any one of the variables leads to the same order of magnitude change in the cost function. As an example, consider the scenario where engine failure occurs while cruising at a forward speed of 40 knots at an altitude of 400 ft. The magnitude of the thrust coefficient used just before engine failure is on the order of 0.003. Rotor speed before engine failure is 354 rpm. The different units used by the state and control variables, and the range of magnitude that these variables will assume in subsequent autorotative descent, clearly indicate the need to normalize and to scale.

To normalize the equations of motion, we use the quantities Ω_0 and R. Here, Ω_0 is the nominal angular speed of the rotor and R the rotor radius. Scaling factors of 10, 100, etc. are used for convenience. Nondimensionalized and scaled quantities for the time, states, and controls used in the analysis are defined as follows

Normalized time

$$\tau = (\Omega_0 t)/100 \quad (12)$$

Normalized states

$$x_1 = w/(0.01\Omega_0 R), \quad x_2 = u/(0.01\Omega_0 R),$$

$$x_3 = (\Omega/\Omega_0), \quad x_4 = h/(10R), \quad x_5 = x/(10R) \quad (13)$$

Normalized controls

$$u_1 = 10^3 C_{T_z} \qquad u_2 = 10^3 C_{T_x} \quad (14)$$

Nonlinear Optimization Problem with Path Inequality Constraints

The helicopter is assumed to be in equilibrium level flight at the time of engine failure with rotor speed Ω_0, forward speed u_0, and height h_0. The optimization problem is to arrive at the ground with small vertical and horizontal velocities subject to maintaining acceptable conditions during the autorotative descent. The cost function of the problem can therefore be taken as the weighted sum of the squared normalized sink-rate and forward speed at the time of touchdown

$$I = \tfrac{1}{2}(x_{1f}^2 + W_x x_{2f}^2) \tag{15}$$

Here W_x is a weighting factor. Acceptable vertical sink-rate at touchdown that is compatible with the shock absorption capability of typical landing gear design is on the order of 8 fps.[1] An acceptable value for forward speed at touchdown is 3 knots.[1] Therefore the value of W_x was taken as 2.5.

The equivalent profile drag coefficient of the rotor increase sharply when the rotor thrust coefficient exceeds the stall limit $(C_T/\sigma)_{\text{stall}}$.[6] The immediate effect of this increase in profile drag is a reduction in the rotor speed [see Eqs. (4) and (5)]. Some of the available rotational energy of the main rotor is therefore wasted via the increased profile power loss. To avoid this condition, the thrust coefficient must be constrained to operate below its stall limit, and this can be achieved with a path inequality constraint.

A value of $(C_T/\sigma)_{\text{stall}} = 0.15$ typical for the OH-58A helicopter is used here. The path inequality constraint in its nondimensional form is

$$\sqrt{u_1^2 + u_2^2} \le \bar{C}_{T_z} \tag{16}$$

where $\bar{C}_{T_z} = (10^3 C_T)_{\text{stall}} = 10^3 (C_T\sigma)_{\text{stall}} \times \sigma$.

In addition to this control inequality constraint, a state inequality constraint was incorporated to impose an upper bound on the vertical sink-rate of the helicopter. This was found necessary since the optimal control program usually results in a very high maximum sink-rate. The maximum permissible sink-rate used was 1800 fpm. The nondimensionalized equivalent of this constraint is formulated as

$$x_1 \le x_{1m} \tag{17}$$

Alternatively, since high sink-rates appear to be a consequence of high rotor speeds, we can place an upper bound on rotor rpm. During the helicopter deceleration phase, optimal control involves a substantial rearward component of rotor thrust which tends to overspeed the rotor. This causes unacceptable blade centrifugal stresses, and pilots are usually instructed to maintain rotor rpm below a maximum operating limit during autorotation.[9] This optimal landing problem with a limit on rotor rpm forms part of our continuing research.

We have posed thus far an optimal control problem with an unspecified terminal time τ_f. The problem may be converted into one with a specified terminal time through the following (further) normalization of the dimensionless time τ:

$$\xi = \tau/\tau_f \tag{18}$$

This transformation changes the independent variable from τ to ξ, which now varies from 0 to 1. If we denote the differentiation with respect to ξ by

$$(\,)' = \frac{\mathrm{d}}{\mathrm{d}\xi} = \tau_f \frac{\mathrm{d}}{\mathrm{d}\tau} = \frac{100\tau_f}{\Omega_0}\frac{\mathrm{d}}{\mathrm{d}t} \tag{19}$$

then the final form of the helicopter optimization problem is

$$\min_{u_1,u_2,\tau_f} I = \tfrac{1}{2}(x_{1f}^2 + W_x x_{2f}^2) \tag{20}$$

subject to

$$x_1' = \tau_f(g_0 - m_0(u_1 x_3^2 + \bar{f}x_1\sqrt{x_1^2 + x_2^2})) \tag{21}$$

$$x_2' = \tau_f m_0(u_2 x_3^2 - \bar{f}x_2\sqrt{x_1^2 + x_2^2}) \tag{22}$$

$$x_3' = -\tau_f i_0 x_3^2 (c_0 + \lambda\sqrt{u_1^2 + u_2^2}) \tag{23}$$

$$x_4' = 0.1\tau_f x_1 \tag{24}$$

$$x_5' = 0.1\tau_f x_2 \tag{25}$$

The initial condition of the state vector is given by

$$X_0 = (0,\bar{u}_0,1,0,0)^T \tag{26}$$

The path inequality constraints on the control and state vectors are

$$\sqrt{u_1^2 + u_2^2} \le \bar{C}_{T_z} \tag{27}$$

$$x_1 \le x_{1m} \tag{28}$$

and the terminal constraints are

$$x_{4f} - \bar{h}_f = 0 \tag{29}$$

$$x_{5f} - \bar{d}_f = 0 \tag{30}$$

where g_0, m_0, $\bar{f}$, i_0, c_0, $\bar{u}_0$, $\bar{h}_f$ and $\bar{d}_f$, as well as a complete derivation of the nonlinear optimization problem can be found in Ref. 10.

Numerical Solution Techniques

Analytical solutions of dynamical optimization problems are only possible when the system equations, the performance index, and constraints of the problem are very simple. Optimal solution of practical engineering problems, like this one, can only be found numerically. One of the earliest attempts at numerical solution of optimal programming problems with control or state inequality constraints was made by Bryson et al.[11] Similar problems had also been treated by several investigators through the use of penalty functions.[12]

Jacobson et al.[13] used a Valentine-type slack variable to convert a state variable inequality constraint into an equality constraint. Using this equality constraint, the original control problem with a state variable inequality constraint is transformed into an unconstrained one of increased dimension. A major difficulty arises when this approach is used on problems where the number of state bounds (r) does not equal the dimension of the control vector (n). In particular, if $n < r$, then one cannot express the controls u as functions of the r slack variables (u_3 in Eq. (31) is an example of a slack control variable, and x_6 in Eq. (32) is an example of a slack state variable). The problem can be bypassed if we instead add path equality constraints to the original problem to enforce the state/control bounds. These path equality constraints are again obtained using the Valentine device. In this way, nonlinear optimal programming problems with path inequality constraints can be transformed into problems with path equality constraints.

Using this approach, we first convert the path inequality constraints [Eqs. (27) and (28)] into equality constraints

$$u_1^2 + u_2^2 + u_3^2 = \bar{C}_{T_z}^2 \tag{31}$$

$$x_1 - x_{1m} + x_6^2 = 0 \tag{32}$$

where u_3 and x_6 are slack control and state variables, respectively. The first derivative of Eq. (32) with respect to ξ is

$$x_1' + 2x_6\tau_f u_4 = 0 \tag{33}$$

where u_4 is an auxiliary control variable defined as

$$\tau_f u_4 = x_6' \tag{34}$$

Finally, substitution of Eq. (21) into Eq. (33) gives the required path equality constraint

$$g_0 - m_0(u_1 x_3^2 + \bar{f} x_1 \sqrt{x_1^2 + x_2^2}) + 2x_6 u_4 = 0 \qquad (35)$$

The helicopter optimization problem with path equality constraints [Eqs. (31) and (35)] is then solved using the Sequential Gradient Restoration technique developed by Miele et al.[7]

Analytical Results

Most helicopters have regions of operation from which a safe autorotational landing cannot be executed. These regions are commonly illustrated with a height-velocity restriction diagram. Typically there are two restriction regions for conventional helicopters. The low speed region is described by the high hover point, the low hover point, and the knee or the highest speed point. In the restricted high speed region there is insufficient clearance between the tail boom and the ground to allow flare to decelerate the helicopter and control rotor rpm prior to ground contact. In order to study autorotational landings from conditions within the high speed region, the point-mass model must be replaced by a rigid body model. Only optimal landing results from conditions within the restricted low speed region are given here.

Optimal Landing of a Helicopter Initially in Hover

Both flight tests and analysis indicate that an initial forward speed improves the autorotational characteristics of a helicopter. Therefore, we first give the optimal control results for the most critical case of descent from engine failure in hover. This is the case considered by Johnson[5] and was found to involve only a pure vertical descent. However, instead of enforcing a hard bound on the thrust coefficient C_T, Johnson included a "penalty" term in the profile power loss of the rotor which increases sharply as the loading is raised above the stall limit. The advantage of Johnson's approach is that it avoids the use of a path inequality constraint. However, the stall limit is usually exceeded using this approach.[5] The following results demonstrate the effectiveness of a "hard" path inequality constraint in enforcing the stall loading limit.

We can simplify the problem if we know or assume that the optimal flight path is vertical. The simplified problem, involving only three states (vertical sink-rate, vertical height, and angular speed of rotor), and one control variable C_{T_z} is given in Ref. 10. As an example case, optimal results for a low altitude autorotation from an initial height of 50 ft were computed, and then compared with an actual autorotation documented in Ref. 2.

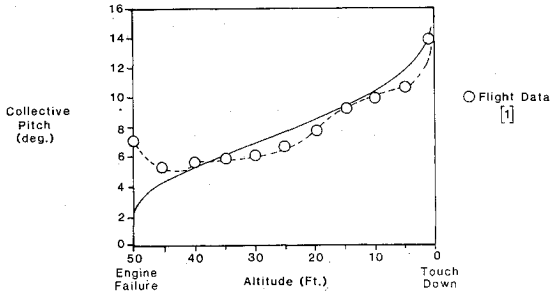

Fig. 3 Comparison of computed collective pitch with flight data.

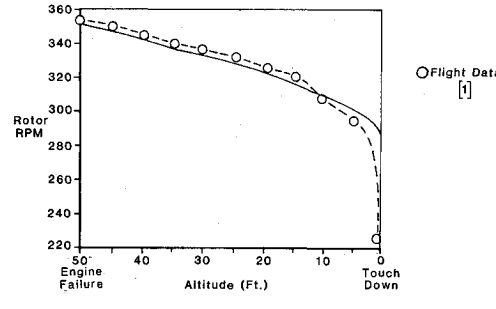

Fig. 4 Comparison of computed rotor rpm with flight data.

Before making any comparison, we must first note that the autorotation technique used in the flight tests differed from the optimal formulation. In flight tests, some forward speed and cyclic flare were involved in order to avoid a vertical descent into the rotor's own wake. Also, for the flight tests reported in Ref. 2, the pilot's primary objective was to attain a zero sink-rate at touchdown and to accept any safe horizontal speed. The technique used is to level the aircraft a few feet above the ground with nearly zero rate of descent. The helicopter then gradually sinks to the ground while small amounts of aft cyclic are applied to reduce the horizontal speed. The technique consistently yields a zero rate of descent at touchdown, but both the flight time and the forward speed at touchdown are usually larger than that given by the optimal program.

Figure 3 compares path histories of the collective pitch calculated by the optimal program (from here on called the computed result) and recorded from flight. Both the computed result and the flight data are given for the case with $\gamma = 2.61$ (i.e., high inertia rotor system). There are differences in collective control immediately following engine failure that reflect details of piloting technique, power transients associated with simulated engine failure, and other autorotation entry issues, but thereafter the agreement is quite good.

Figure 4 compares the rotor angular speed histories. The agreement is also quite good, but the recorded rotor speed at touchdown is 220 rpm compared to the computed result of 268 rpm. This indicates that the optimal program uses less energy in the landing maneuver than the pilot, who seeks to exploit all available rotor energy to achieve touchdown at nearly zero sink-rate.

Figure 5 shows the computed time histories of C_T/σ for four entry heights of 25, 50, 100 and 200 ft. As the entry height is increased, we see a corresponding increase in the amount of (normalized) time that the thrust coefficient spends on its stall limit. This trend continues until the entry height of 100 ft is reached. Above this "critical" height of 100 ft, further increase in entry height actually reduces that time since there is now greater opportunity to reduce collective at the beginning of the maneuver, thereby preserving rotor speed for the final landing. Above or below this most critical entry height (MCEH), the autorotational landing maneuver becomes progressively easier to execute.

Further indication of this hypothesis of a MCEH for the optimal calculation is found in the rotor speed time histories shown in Fig. 6. Since the sink-rates at touchdown for all entry heights considered are small, we cannot use them to effectively judge the criticality of the landings. However, we do know that the lower the rotor rpm at touchdown, the greater the amount of energy used in the landing maneuver. Therefore, one easy way to show the existence of the MCEH is to plot the rotor speed at touchdown against the corresponding entry height. Such a plot is given in Fig. 7, which shows that the maximum extraction of rotational energy occurs around an entry height of 100 ft.

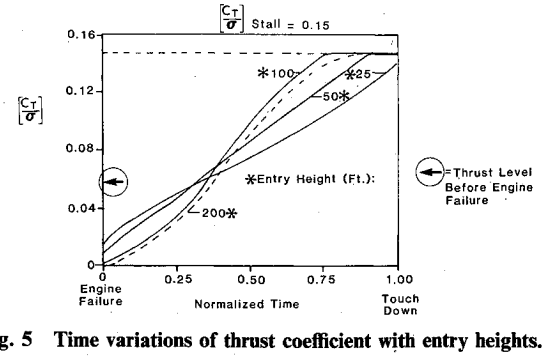

Fig. 5 Time variations of thrust coefficient with entry heights.

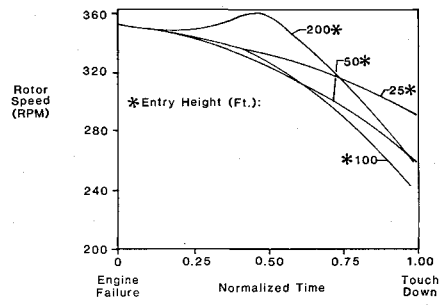

Fig. 6 Time variations of rotor rpm with entry heights.

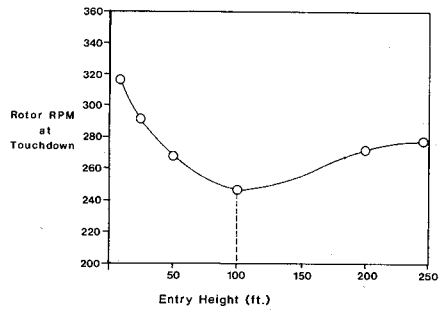

Fig. 7 Variations of touchdown rotor rpm with entry height.

Optimal Landing of a Helicopter in Forward Flight

For the forward flight cases, the HERS model (see Table 1) with a rotor having a Lock Number γ of 4.38 is used for the analysis. Entry conditions studied are summarized in Fig. 8. Note that entry conditions 1, 2 and 6 are the same altitude of 100 ft but with different entry speeds. Similarly, entry conditions 1, 5 and 4 have (approximately) the same forward speed of 8 knots but are at different entry heights. In this way, effects of both the entry speed and altitude can be studied.

Results for a simulated engine failure of the HERS flight test vehicle (with $\gamma = 5.43$) at the "knee" of the H-V diagram (115 ft altitude and 45 knots) are used for comparison. The computed results are those obtained for entry condition 2, i.e., 38 knots and 100 ft. One must note these differences in rotor inertia and entry conditions when making comparisons.

Figure 9 compares the collective pitch time histories. The comparison is reasonably good. The most obvious difference between these time histories is the lower collective pitch control used in flight tests. This difference is partly due to the fact that the helicopter landed with a forward speed of 20 fps in test instead of a few fps found in the optimal program. As a result, the computed rotor rpm is lower than that found in the actual flight test (see Fig. 10). With the higher rotor rpm, relatively lower collective pitch was used in flight test to generate the needed thrust.

Optimal time histories of C_{T_x} and C_{T_z} for entry speeds of 12, 38, and 57 knots, all at the same entry height of 100 ft are compared in Fig. 11. Note the variation in the C_{T_x} program with the entry speed. When the entry speed is relatively low (e.g., 12 knots), forward cyclic is used to accelerate the helicopter to a faster speed before aft cyclic is used to slow it down for touchdown. At an intermediate speed of 38 knots, there is only a brief period of forward acceleration. With a high entry speed of 57 knots, aft cyclic must be applied immediately after engine failure in order to decelerate the helicopter in time for the final touchdown.

These results reflect the variation in parasite and induced drag with airspeed, which is characteristic for all aircraft and responsible for the existence of a speed for minimum steady-state energy dissipation. For the OH-58A helicopter used in the study, that speed was shown in Fig. 2 to be about 45 knots. Although the transient nature of the optimal results precludes

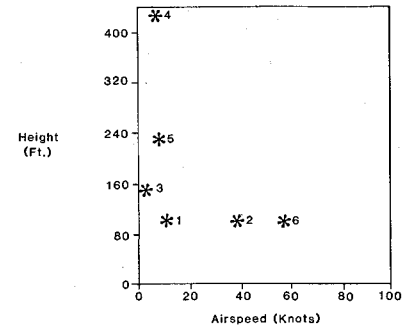

Fig. 8 H-V entry conditions.

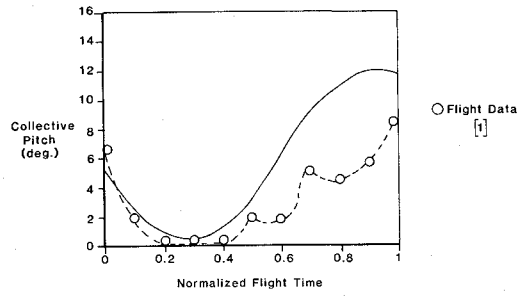

Fig. 9 Comparison of computed collective pitch with flight data.

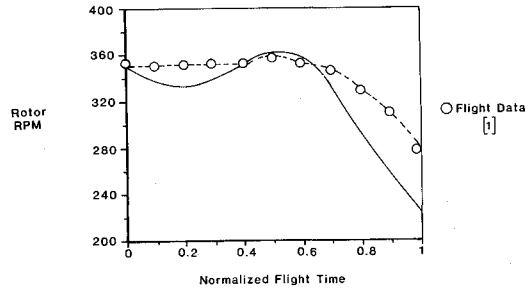

Fig. 10 Comparison of computed rotor rpm with flight data.

direct inference, it is not surprising that the optimal program avoids both high and low speeds where total energy dissipation is high.

Optimal Landing Program with a Descent Velocity Bound

The entry condition selected for this study is condition 4 in Fig. 8 (with $\gamma = 4.38$). Without a descent velocity bound, the optimal trajectory with this entry condition results in unacceptably high peak descent velocity, which in turn, results in rotor overspeeding. With a descent velocity bound, the optimal time variation of the descent velocity will resemble that shown in Fig. 12. The helicopter starts initially with a zero rate of descent. This rate then increases and touches and stays on its upperbound for a period of time. Finally, the rate of descent is reduced to allow for a soft touchdown.

A value of 1800 fpm was selected as the maximum permissible sink-rate and the optimal time variations of C_{T_z} and C_{T_x}, are given in Fig. 13.

With reference to the C_{T_z} time histories, there is an enforced division of the autorotation maneuver into three phases. The entry phase consists of a sharp drop in the thrust coefficient in order to preserve the rotor rpm. This is followed by a steady increase in the thrust until a steady state value of $C_T/\sigma \doteq 0.08$ is reached. This thrust level is then maintained over the steady descent phase. The landing maneuver ends with a rapid increase in the collective pitch when touchdown is imminent.

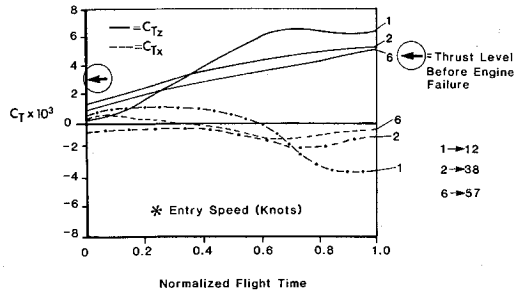

Fig. 11 Variations of horizontal and vertical thrust coefficients with entry speed (entry height = 100 ft).

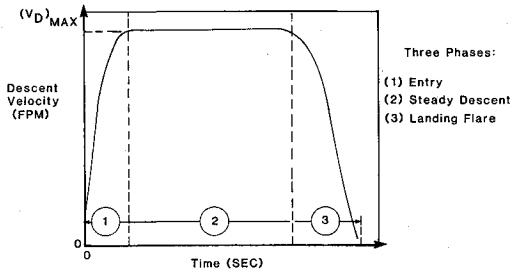

Fig. 12 Typical time variation of the descent velocity.

This clear division of the landing maneuver is a distinct feature of the present control program. These control phases resemble those practiced by helicopter pilots in their autorotational training.

Differences in the time variations of the main rotor rpm in cases with and without the bound are depicted in Fig. 14. Without the bound, the peak rotor speed is about 30% higher than its nominal value of 353 rpm. This causes unacceptable blade centrifugal stresses. Figure 14 shows that this "peaking" in the rotor rpm has been suppressed with the descent velocity bound. The peak angular speed for the case with the bound is actually less than the nominal speed. Therefore the "peaking" of the rotor rpm could be removed either directly with the addition of an inequality constraint on the rotor rpm or indirectly through the bounding of the descent velocity.

Concluding Remarks

A point-mass model of an OH-58A helicopter was used to determine autorotation profiles that minimize touchdown velocity with bounds on rotor thrust and descent velocity. The optimal solutions exhibit control histories similar to those used by pilots in autorotational landings. The study indicates that there is the potential for a substantial reduction in the H-V restriction zone using optimal control techniques.

There are many practical problems in applying optimal energy management techniques to helicopter autorotation, such as 1) measuring and incorporating the effects of wind, wind shear, and turbulence, 2) displaying calculated control commands to the pilot, or executing them with an autopilot, 3) designating desired or acceptable touchdown locations, 4) calculating and displaying achievable landing footprints within which the pilot can continuously select satisfactory touchdown sites, and 5) meeting on-line computational requirements. In addition, there are considerations of flight safety and pilot acceptance. Nevertheless, there seems to be potential for these techniques in calculating a priori the height-velocity restriction curve, as well as assisting the pilot and enhancing safety in one of the most difficult of all piloting tasks.

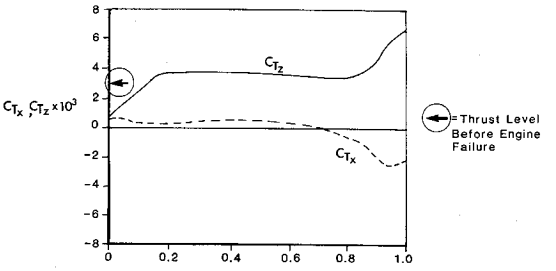

Fig. 13 Time variations of thrust coefficients with a descent velocity bound.

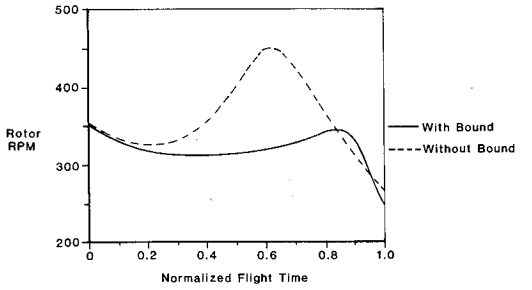

Fig. 14 Time variations of rotor rpm with and without a descent velocity bound.

Acknowledgments

The first author is indebted to William A. Decker and Dr. Robert T. Chen, both at NASA Ames Research Center, for many helpful discussions. The research was supported by NASA Grant NCC2-106.

References

[1]Wood, T. L., "High Energy Rotor System," presented at the 32nd Annual National Forum of the American Helicopter Society, Paper 1014, Washington, D.C., May 1976.

[2]Dooley, L. W. and Yeary, R. D., "Flight Test Evaluation of the High Inertia Rotor System," USARTL-TR-79-9, June 1979.

[3]Graves, J. D., "Methods and Devices to Improve Helicopter Autorotational Characteristics," USARADCOM TR-82-D-38, Sept. 1983.

[4]Pleasants, W. A. III and White, G. T. III, "Status of Improved Autorotative Landing Research," *Journal of American Helicopter Society*, Vol. 128, No. 1, Jan. 1983.

[5]Johnson, W., "Helicopter Optimal Descent and Landing after Power Loss," NASA TM 73,244, May 1977.

[6]Gessow, A. and Myers, G. C. Jr., *Aerodynamics of the Helicopter*, Frederick Ungar Publishing Co., New York, 1952.

[7]Miele, A. et al., "Sequential Gradient-Restoration Algorithm for Optimal Control Problems with Non-differential Constraints," *Journal of Optimization Theory and Applications*, Vol. 13, No. 2, Feb. 1974.

[8]Jacoby, S., *Iteration Methods for Nonlinear Optimum Control Problems*, Prentice-Hall, Englewood Cliffs, NJ, May 1972.

[9]*Operator's Manual, Army Models OH-58C Helicopter*, Tech. Manual 55-1520-235-10, Headquarters, Department of the Army, Washington, D.C., April 1978.

[10]Allan Y. Lee, "Optimal Landing of a Helicopter in Autorotation," Ph.D. thesis, Department of Aeronautics and Astronautics, Stanford University, Stanford, CA, July 1986.

[11]Speyer, J. L. and Bryson, A. E., Jr., "Optimal Programming Problems with Bounded State Space," *AIAA Journal*, Vol. 6, No. 5, Aug. 1968, pp. 1488–1491.

[12]McGill, R., "Optimal Control Inequality State Constraints, and the Generalized Newton Raphson Algorithm," *Journal of Control and Optimization, Society for Industrial and Applied Mathematics*, (Control), Ser. A, Vol. 3, No. 2, 1965.

[13]Jacobson, D. H. and Lele, M. M., "A Transformation Technique for Optimal Control Problems with a State Variable Inequality Constraint," *IEEE Transactions on Automatic Control*, Vol. AC-14, No. 5, Oct. 1969.